

Discrete conducting states, wave-vector variation, and carrier mobilities in NbSe₃ microsamples

S. G. Zybtev and V. Ya. Pokrovskii*

Kotel'nikov Institute of Radioengineering and Electronics of the Russian Academy of Sciences, 125009 Mokhovaya 11-7, Moscow, Russia

(Received 30 November 2010; revised manuscript received 14 July 2011; published 30 August 2011)

Crystals of NbSe₃ with typical dimensions of $30\ \mu\text{m} \times 0.03\ \mu\text{m}^2$ demonstrate jumps of conductivity induced by temperature changes. The jumps are observed in both charge-density wave (CDW) states, but more detailed studies have been performed for the low-temperature CDW. The jumps reveal single phase-slip events that switch the CDW between discrete states with different wave vectors. Based on this observation, we find the temperature dependencies of the CDW wave vectors and the mobilities of the quasiparticles for type-I and type-III chains. The mobility of carriers originating from the type-I chains (i.e., “pocket” holes) appears to be extremely high, approaching $10^5\ \text{cm}^2/\text{V}\cdot\text{s}$ below 25 K.

DOI: [10.1103/PhysRevB.84.085139](https://doi.org/10.1103/PhysRevB.84.085139)

PACS number(s): 71.45.Lr, 61.44.Fw, 72.20.Fr

I. INTRODUCTION

NbSe₃ is the most thoroughly studied and, in many ways, the most interesting charge density wave (CDW) material because two highly coherent CDWs coexist with metallic electrons down to zero temperature. For more than 30 years, this quasi-one-dimensional and layered compound has been in the focus of scientific attention. At present, questions of topical interest involve surface properties,¹ the interaction between the two CDWs,^{2,3} effects of magnetic field,^{4,5} point contact spectroscopy,⁶ interlayer tunneling,^{6,7} size effects,^{8,9} and CDW deformations and their spatial distributions.¹⁰

In spite of extended studies involving the Angle Resolved Photoemission Spectroscopy (ARPES) technique,¹¹ understanding of the band structure of NbSe₃ and its temperature evolution is far from clear. It is known that in NbSe₃, atoms of niobium form metallic chains of three different types.¹² The upper CDW transition at $T_{p1} = 140\ \text{K}$ gaps the carriers over the type-III chains, and the lower transition ($T_{p2} = 59\ \text{K}$) partially gaps carriers over the type-I chains, while the type-II chains are not (or nearly not) affected by the transitions. Consequently, different types of single-particle carriers are present in NbSe₃, and it is rather difficult to distinguish their contributions to transport properties. Here, we face a general problem for (semi)conductors with complex band structure.

The two-band model,¹³ based on studies of the Hall effect, transverse magnetoresistance, and conductivity anisotropy, was a courageous attempt to solve this problem. The author of the model asserted extremely high mobility of the remnant metallic (pocket) conducting particles. However, the simulation¹³ seems to be model-sensitive: The resulting mobility estimates are based on a six-parameter fit. The carriers on type-II chains were not taken into account. The simulation strongly modifies the result of “direct” measurements of effective mobility, determined as the square root of the coefficient of B^2 in the expansion of the magnetoresistivity.¹⁴ This difference illustrates that the “direct” method can give only a very rough estimate of mobility due to averaging over different-type carriers.

Recently results and predictions of the two-band model¹³ have been reconsidered.⁵ It has been shown that for the low-temperature CDW, there are two qualitatively different kinds of normal metal carriers: The first carriers are the

heavy electrons originating from the ungapped type-II chains. Another type of carriers, holes, originate from the type-I chains and form pockets; their effective mass can be very small. However, quantitative estimates of the mobilities for each type of carrier have not been done yet. Thus, to date, no direct experiments are available that provide the mobilities of carriers in NbSe₃.

Here, we propose a completely different experimental approach that gives direct information on the mobilities of the main carriers. Roughly speaking, we provide a calibrated “injection” of the particular carriers and then measure the conductivity change.

To understand the idea of the approach, we should turn to such basics of the CDW as metastability, phase slippage, and their specifics in microscopic samples. A feature of many CDW compounds is the temperature dependence of the wave vector, q . The q change requires overcoming a barrier for a phase slip (PS) in order to produce or annihilate a CDW wave length. Consequently, the q -vector falls behind its equilibrium value. Because relaxation of q towards equilibrium goes extremely slow, such states are considered to be metastable. Each PS event adds/removes two electrons per chain, or, more exactly, transfers them between the CDW and the single-particle states. Therefore, the hysteretic change of the q -vector with temperature unmasks itself in the variations of single-particle conductivity and other transport properties.^{12,15}

If the CDW is coherent over the cross section, and the sample is short enough, one can distinguish discrete steps of conductivity associated with single PS events, as was found for TaS₃¹⁶ and K_{0.3}MoO₃ (the blue bronze [BB]).¹⁷ In the case of BB, one can observe a sort of quantization of the conducting states and regular in temperature transitions between them.¹⁷

Each PS event changes the *average* value of q by $\pm 2\pi/L$, where L is the sample length. The corresponding change of quasiparticle concentration per conducting chain, δn , is $\pm n_c/L$, where n_c is the number of condensed electrons per CDW wavelength, usually taken as 2. In the case of unipolar conduction, one will observe a step of specific conductivity $\delta\sigma_s = e\mu\delta n/s_0$, where e is the elementary charge, and s_0 is the area per conducting chain. Knowing δn and $\delta\sigma_s$, one can directly find the carriers' mobility, μ .¹⁷

$$\mu = \delta\sigma_s L s_0 / (2e) = \delta\sigma L^2 s_0 / (2es), \quad (1)$$

where $\delta\sigma = \delta\sigma_{s,s}/L$ is the value of conduction step, and s is the cross-sectional area of the sample. The bullet point here is that Eq. (1) gives the mobility of the carriers originating from *particular* chains, i.e., the CDW chains where the quasiparticles were generated or annihilated through a PS event. This is especially important for NbSe₃, where different-type Nb chains give rise to different electronic bands.

If conductivity is not purely unipolar, Eq. (1) gives an estimate from the bottom.

The picture of discrete conducting states and jumps between them¹⁷ has allowed reconstruction of the $q(T)$ dependence for BB; it appears to be in agreement with the diffraction studies and exceeds them in resolution. The mobility obtained from the value of $\delta\sigma$ nearly coincides with the value provided by the Hall-effect studies.¹⁸

TaS₃ and K_{0.3}MoO₃ are completely dielectric in the CDW state. As for NbSe₃, the contributions of metallic bands bridge the gapped quasiparticles. This complicates observation of hysteresis and steps of conductivity in this compound. On the other hand, the expected high mobility of quasiparticles at low temperatures^{5,13} could save the situation.

Previously, hysteresis in conductivity, up to 4%, has been observed only below T_{P2} .¹⁹ However, there are no reports concerning temperature variations of the wave vector, q_2 , for the lower CDW state, which could be responsible for the hysteresis. The wave vector variation, $q_1(T)$, has been found only for the upper CDW state.²⁰ However, hysteresis in σ is nearly absent above 60 K.¹⁹

In our paper, we report the first observations of discrete conducting states in small samples of NbSe₃. The jumps between them, i.e., single PS events, are provoked by the temperature-induced change of q_2 . From the temperature distribution of the PS events, we reconstruct the $q_2(T)$ dependence, which has not been observed with diffraction techniques up to now. The jumps observed also provide the value of mobility of the quasiparticles from the type-I chains, which are partially gapped through the formation of the lower CDW. The resulting mobility appears to grow at low temperatures, in agreement with Ref. 13, or even faster. We also report observation of single PS events and thermal hysteresis of conductivity for the *upper* CDW state.

II. EXPERIMENTAL DETAILS

We selected thin samples of NbSe₃ from a high-quality batch. The quality was confirmed by the ratio of resistances, $R(300\text{ K})/R(4.2\text{ K})$, known as residual resistance ratio (RRR).¹² To rule out the size effects,⁸ we tested a bulk sample with cross-sectional area about $250\ \mu\text{m}^2$ from the same batch. Figure 1 shows the temperature dependence of resistance of this sample, $R(T)$. We found RRR to be 160, which is large enough to characterize the batch as a good one (see Refs. 12, 21, and 22 for comparison).

To resolve the steps of conductivity, $\delta\sigma$, one should take short samples, because $\delta\sigma/\sigma$ scales as $1/L$.^{16,17} However, as we will see below, the $q_2(T)$ dependence appears very weak. Thus, we are caught between two contradictory requirements: Shortening a sample, we increase $\delta\sigma/\sigma$ but lose the number of steps in the same temperature range. As a compromise, we took samples 30–60 μm long.

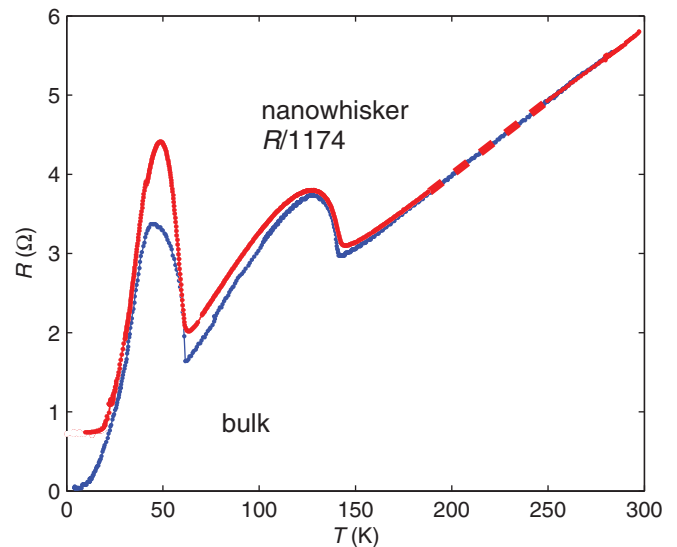


FIG. 1. (Color online) Temperature dependencies of resistance for the bulk NbSe₃ sample and for a microsample (No. 5: $L = 62\ \mu\text{m}$, $R_{300} = 6.7\ \text{k}\Omega$). For the microsample, the resistance is divided by 1174.

The samples must also be thin enough, so that a PS event will cover the whole cross section of the whisker. However, the resistivity of the samples with $s \leq 0.1\ \mu\text{m}^2$ is substantially increased at low temperatures, whereas still thinner samples ($s \leq 0.01\ \mu\text{m}^2$) tend to dielectric behavior.^{8,24} Because we did not want to obtain characteristics specific only for the thin samples, we found the optimal cross-sectional area of the samples to be about $(2 \div 4) \times 10^{-2}\ \mu\text{m}^2$. A rescaled $R(T)$ dependence for a typical microsample is also shown in Fig. 1. The increase of low-temperature resistivity in comparison with the bulk sample is clearly seen, in accordance with Ref. 8. For the samples in our study, the RRR varied between 5 and 10. However, as one can see from Fig. 1, for $T > 20\ \text{K}$, the increase of the resistivity of the microsample is within a factor of 1.5. From this, we can conclude that for $T > 20\ \text{K}$, the values of μ are approximately the same (within a factor of 1.5) for the microsamples and bulk samples. Thus, we can expand the central result of our studies, the low-temperature growth of mobility (see Fig. 6 below), for the bulk samples.

The effective length of each sample was set by a pair of gold contacts deposited with the laser-ablation technique, which is likely to provide tight boundary conditions for the CDW.¹⁷ Four-probe measurements of contact resistance, R_c , excluding the resistance of the leads,²⁵ were performed; temperature dependence of the contact resistance is shown in Fig. 2. The sample width is $1.2\ \mu\text{m}$, the length of the golden strip is $13\ \mu\text{m}$, and so the contact area is $16\ \mu\text{m}^2$. From Fig. 2, one can see that the value of the contact resistivity is of the order of $10^{-8}\ \Omega\ \text{cm}^2$. This value is negligible for our measurements within the whole temperature range. Note that the temperature dependence of the contact resistivity shows metallic behavior, indicating absence of a dielectric barrier under the contact.

The high quality of the batch is justified also by the current-voltage characteristics of the samples. For the bulk sample, the threshold field is found to be $56\ \text{mV/cm}$ at $120\ \text{K}$ and

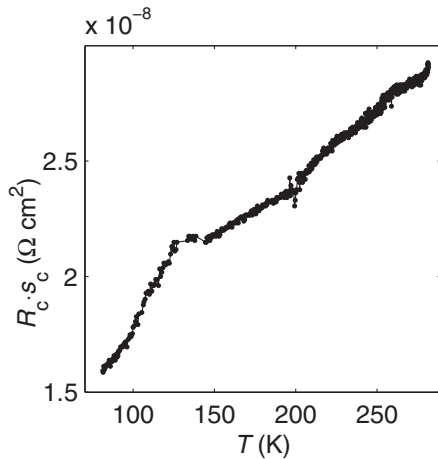


FIG. 2. Temperature dependence of the contact resistance, R_c , multiplied by its area, s_c ; $s_c = 1.2 \times 13 \mu\text{m}^2$ ($1.2 \mu\text{m}$ is the width of the sample; $13 \mu\text{m}^2$ is the length of the golden strip). The resistance is the same for currents 2×10^{-5} and 2×10^{-6} A.

6 mV/cm at 47 K. These are rather low values (for comparison, see Ref. 12, p. 195).

For the microsamples studied in this paper, the threshold field is higher, in accordance with the size effect.^{9,23} The sharp depinning of the CDW at the threshold indicates high coherence of the CDW. Figure 3 gives an example of current dependencies of differential resistance, $R_d(I)$, for one of the microsamples at 120 K. The Shapiro steps,¹² or more exactly, the peaks of R_d , in Fig. 3 indicate nearly complete synchronization of the CDW under 50 MHz irradiation.

The conductivity was measured with the conventional lock-in technique using an SR830 amplifier. The alternating current (AC) was within 10% of the threshold value. This means that the voltage across the samples, V , was typically 1 mV

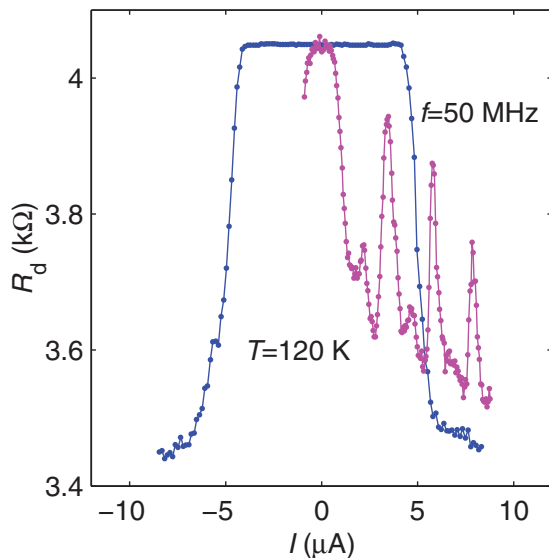


FIG. 3. (Color online) $R_d(I)$ dependence for one of the microsamples (No. 7: $L = 50 \mu\text{m}$, $R_{300} = 6.4 \text{ k}\Omega$) at 120 K as it is and under 50 MHz irradiation. The threshold field is about 3 V/cm. At the present power of radiation, the threshold field is suppressed, but $R_d(0)$ is unchanged.

or less, and it had to be measured accurately enough to resolve steps of voltage down to $\delta V/V = 0.1\%$ (for the upper CDW). The instabilities of the lock-in amplifier and of the contact resistance were also kept below this value, 0.1%, for several hours, i.e., the time necessary for the measurements. Such a long time was necessary to pass the maximum possible number of metastable states in a wide temperature range. To control the stability during the measurements, the samples were several times heated above the Peierls transition, where metastability is absent. In this way, we made sure that the readings of the lock-in had not drifted away. After this manipulation, the samples were cooled back, and the measurements continued. The results presented here are based on studies of nine NbSe_3 samples.

III. EXPERIMENTAL RESULTS AND DISCUSSION

The most detailed measurements were performed for the lower CDW state. Figure 4 shows a fragment of resistance-temperature dependence, $R(T)$, for sample No. 1 in the range 34–57 K. Hysteresis of resistance within 4% can be seen, in agreement with Ref. 19. Note that the resistance is lower for the cooling curve. This is typical for the completely gapped CDW conductors, say, TaS_3 , $\text{K}_{0.3}\text{MoO}_3$. For NbSe_3 with $dR/dT > 0$ ($T < 47$ K), this means that R goes *ahead* of its equilibrium value, i.e., the hysteresis looks abnormal. Still, this is not very surprising because the hysteresis comes from the contribution of the dielectric conducting channel, for which $dR/dT < 0$.

Looking at the $R(T)$ dependence in Fig. 4, one can also notice jumps of resistance. The jumps look similar with those observed for nanosamples of TaS_3 ¹⁶ and BB.¹⁷ Like in these compounds, the jumps of resistance are directed upward over the cooling curve and downward over the heating curve, i.e., toward the middle of the hysteresis loop.

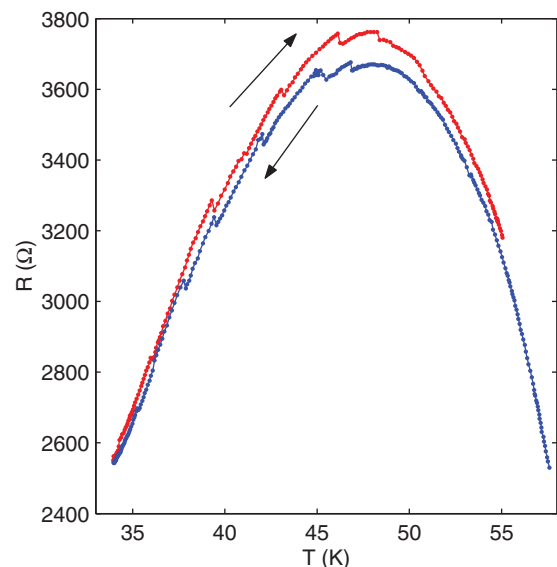


FIG. 4. (Color online) $R(T)$ dependence for the sample No. 1 in the range of the lower CDW state. $L = 35 \mu\text{m}$, $R_{300} = 5.1 \text{ k}\Omega$.

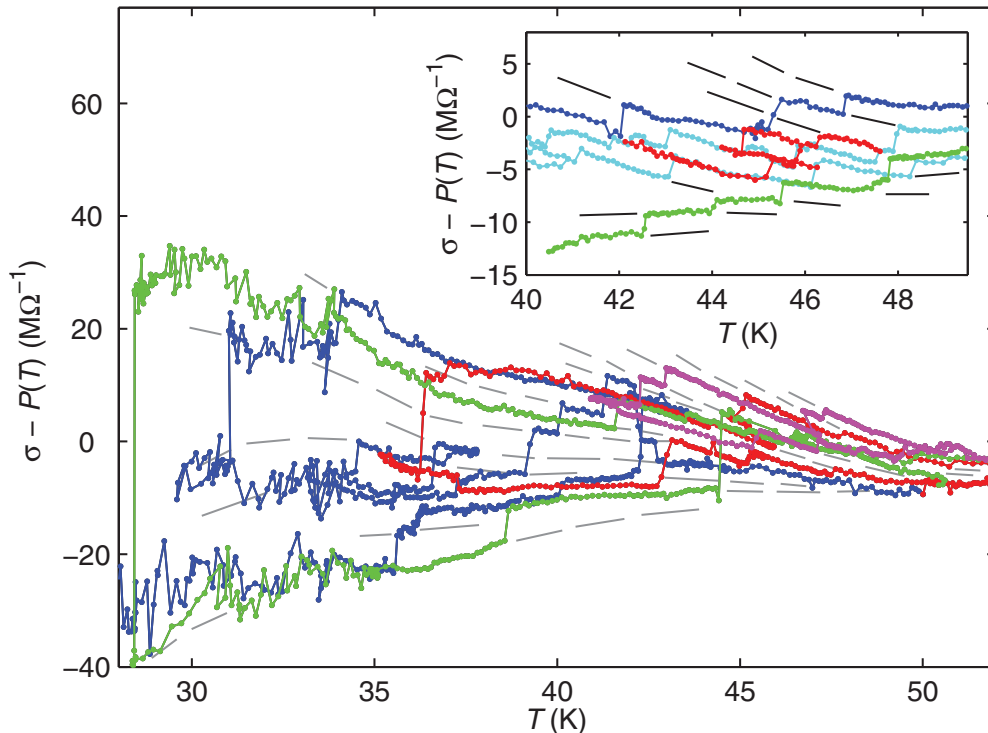


FIG. 5. (Color online) The value of $\sigma(T)$ after subtracting a polynomial for the sample No. 2 ($L = 33 \mu\text{m}$, $R_{300} = 3.2 \text{ k}\Omega$). The polynomial fit is the same for all the curves. The broken lines are guides for the eye showing the missed reversible fragments of the curves. The inset shows a similar presentation for sample No. 1 in a narrow temperature range.

The jumps provide transitions between discrete conducting states. To make the states more visible, we subtracted polynomial approximations, $P(T)$,²⁶ from the $\sigma(T)$ curves. Examples of the curves obtained this way are shown in Fig. 5 and in the inset to Fig. 5. The discrete conducting states are clearly seen. The broken lines, guides for eye, help to trace the missing reversible fragments of the curves. The whole picture of discrete states and jumps between them is closely analogous with those observed for TaS_3 ¹⁶ and BB .¹⁷ Therefore, we conclude that the conductivity jumps are single PS events.

The conducting states and the jumps between them can be resolved down to approximately 20 K. At lower temperatures, the value of error in $\delta\sigma$ appears too large.

From the distribution of the steps in temperature, one can find the q_2 change, $\delta q_2(T)$.¹⁷ The results for $q_2(T)$ change agree for all the samples studied. Only several (typically, $N \approx 4-8$) steps were observed in the whole temperature range below T_{P2} , i.e., between 20 and 50 K. This means that the total q_2 change, $2\pi N/L$, is about $(1-2) \times 10^{-4}$ of q_2 . Evidently, this is the reason why the $q_2(T)$ dependence has not yet been detected using diffraction techniques. In certain cases, it is possible to reconstruct the “quantized” values of q_2 and the hysteresis loop in δq_2 . A fragment of a $q_2(T)$ hysteresis loop for the sample No. 1 is shown in the inset to Fig. 6. Notice that the total q_2 change is comparable with the width of the hysteresis loop in q_2 : From the inset to Fig. 5, one can see that the total loop width for this sample comprises 4–5 jumps.

Knowing $\delta\sigma$, one can find μ from Eq. (1). The value of s was found from the room-temperature resistance and

specific resistivity, $3 \times 10^{-4} \Omega \text{ cm}$. The transverse dimensions were also controlled with an atomic force microscope (AFM). The area s_0 was found as the area of the elementary cell (148 \AA^2)^{12,15} divided by 2 (the number of chains of each type).

In some cases, the steps of conductivity varied in height. This could be attributed to an incomplete, or, *vice versa*, double PS event. To find the single-PS value of $\delta\sigma$ with the best possible accuracy, we did not process individual steps, as was done in Refs. 16 and 17. Instead, we present the repeatedly recorded $\sigma(T)$ dependencies with polynomials subtracted, as demonstrated in Fig. 5. In a wide temperature range, the result looks like a number of lines fanning out at low temperatures. The obvious growth of $\delta\sigma$ with decreasing T reveals the growth of the carriers’ mobility, Eq. (1). To find $\delta\sigma$, we measured the difference of conductivities between a pair of states at the edges of the “fan” and divided it by the number of steps separating them. A probable error in 1–2 steps would not affect the value of $\delta\sigma$ dramatically.

The results of the mobility calculations for different samples are shown in Fig. 6, together with the longitudinal mobilities obtained within the two-band model.¹³ Note that here *no* fitting parameters are involved. One can see drastic growth of the carriers’ mobility at low T . Around 20 K, it achieves $4 \times 10^4 \text{ cm}^2/\text{V}\cdot\text{s}$, and extrapolation to liquid-helium temperatures gives a value well above $10^5 \text{ cm}^2/\text{V}\cdot\text{s}$. Clearly, this is the mobility of the main carriers at the type-I chains. According to Ref. 13, these are the pocket holes, as the contributions of thermally excited quasiparticles could be neglected below 50 K. The mobility of the holes appears to be in agreement with the model around 40 K (see the open circles in Fig. 6)

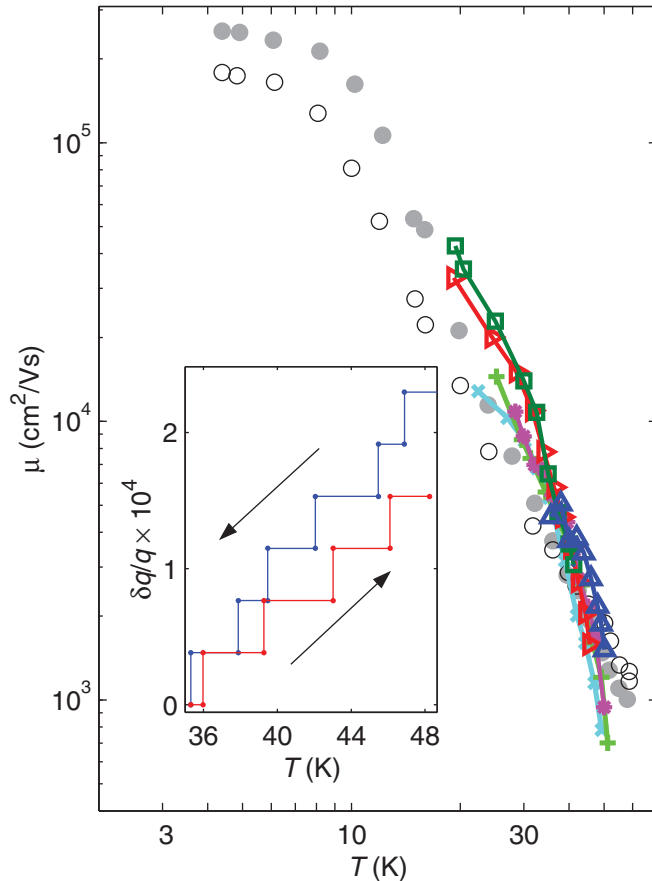


FIG. 6. (Color online) The temperature dependence of mobility obtained from processing of 5 samples ($L = 29\text{--}62\ \mu\text{m}$). Different symbols correspond with different samples: Δ —No. 1 ($L = 35\ \mu\text{m}$, $R_{300} = 5.1\ \text{k}\Omega$), \star —No. 2 ($L = 33\ \mu\text{m}$, $R_{300} = 3.2\ \text{k}\Omega$), \times —No. 3 ($L = 32\ \mu\text{m}$, $R_{300} = 1.4\ \text{k}\Omega$), $+$ —No. 4 ($L = 34\ \mu\text{m}$, $R_{300} = 3.7\ \text{k}\Omega$), \triangleright —No. 5 ($L = 62\ \mu\text{m}$, $R_{300} = 6.7\ \text{k}\Omega$), \square —No. 6 ($L = 29\ \mu\text{m}$, $R_{300} = 4.2\ \text{k}\Omega$). The closed circles (electrons) and open circles (holes) are taken from Ref. 13. Inset: A fragment of $q_2(T)$ change for sample No. 1 restored on the assumption that each jump of σ corresponds with $\delta q = \pm 2\pi/L$ (see Fig. 4 and inset to Fig. 5).

and grows noticeably faster with cooling, as was suggested in Ref. 5. It was also argued⁵ that the pocket holes, having very low effective mass, are strongly different from the thermally excited quasiparticles.

We should note that some of the samples, a minor part, showed a different behavior for resistance, evidently because of some defects in structure. Several samples showed smaller slopes in the $R(T)$ curves near room temperature. Such samples were sorted out. One of the samples with relatively high cross-sectional area, $5 \times 10^{-2}\ \mu\text{m}^2$, showed anomalous dielectrization at the lower transition (RRR around 3–4). It also showed steps of conductivity. The value of mobility calculated from them appears to grow only slightly with cooling and saturates at the level of about $10^3\ \text{cm}^2/\text{V}\cdot\text{s}$ below 45 K. This example indicates drop of the holes' mobility for the samples with higher degrees of dielectrization at low temperatures. However, a special study is needed, involving thinner samples,⁸ to make definite conclusions about the carriers' mobilities in them.

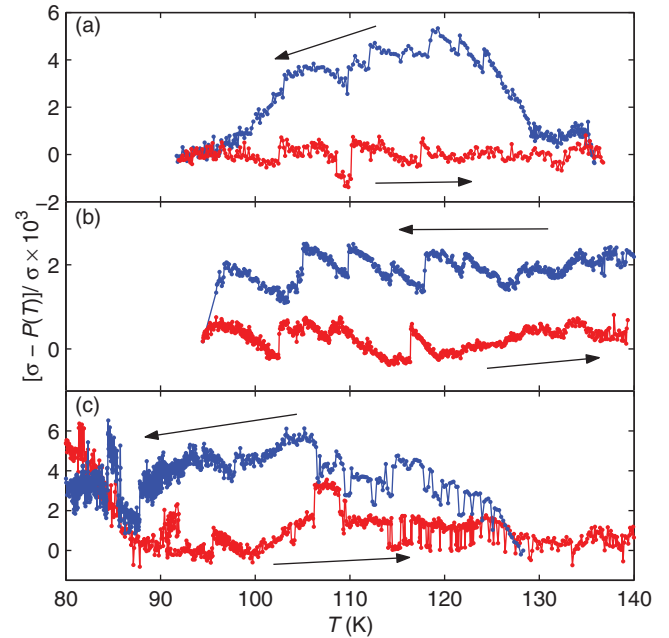


FIG. 7. (Color online) Normalized changes of σ in the range of the upper CDW state. Polynomials approximating the heating part of $\sigma(T)$ are subtracted. The samples are: (a) No. 1, (b) No. 7 ($L = 50\ \mu\text{m}$, $R_{300} = 6.4\ \text{k}\Omega$), and (c) No. 8 ($L = 32\ \mu\text{m}$, $R_{300} = 4.2\ \text{k}\Omega$).

In conclusion, we would like to present our results for the upper CDW state. The conductivity jumps are found in the range 100–130 K. The relative height of the steps appears to be of the order of 10^{-3} , and the relative width of the hysteresis loop in conductivity appears to be $\sim 5 \times 10^{-3}$. These values are rather small and close to the limit of the experimental resolution. The steps could be detected only after processing the data, i.e., after subtraction of the polynomials from the $\sigma(T)$ curves. The resulting dependencies normalized by the average value of σ are shown in Fig. 7 for the three samples studied. One can see that the jumps are directed mainly toward the middle of the hysteresis loops, as it should be for the PS events.

Counting the jumps, we could find the q_1 temperature change. For two samples [Figs. 7(a) and 7(b)], the q_1 change is found to be $3\text{--}6 \times 10^{-4}$. This appears to be several times smaller than the value reported in Ref. 20. The third sample [Fig. 7(c)] demonstrates a still smaller (about 3 times) change of q_1 with T . This sample is remarkable also for the spontaneous switching between the states. Similar switching, spontaneous PS events, have been observed in nanosized samples of TaS₃ not far below the Peierls transition temperature.²⁷

Based on our results, we can suggest that the $q_1(T)$ variation is strongly sample dependent.

The step heights provide the mobility values for the lower CDW state. Because it was difficult to trace the discrete conducting states, we processed individual jumps. The measured values of $\delta\sigma$, as well as the calculated values of μ , are presented in Fig. 8. Evidently, some of the jumps correspond with double PS events; incomplete PSs can also happen. Excluding these anomalous jumps, we find the mobility to be 400–600 $\text{cm}^2/\text{V}\cdot\text{s}$

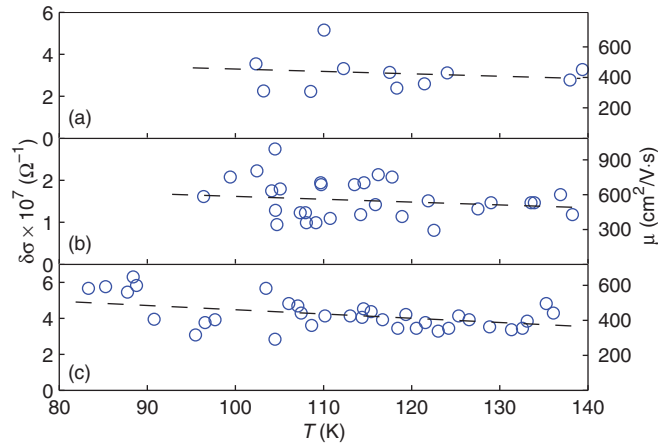


FIG. 8. (Color online) The heights of the jumps of conductivity (left scale) and the corresponding values of mobility (right scale) for the samples presented in Fig. 7.

for all three samples, with a tendency to grow with decreasing T (Fig. 8). This value of μ , relevant to the quasiparticles over type-III chains, is rather high: For comparison, the average room-temperature mobility of electrons in NbSe_3 , given an electron concentration $3.9 \times 10^{21} \text{ cm}^{-3}$ (Ref. 12), is about $5 \text{ cm}^2/\text{V}\cdot\text{s}$. In BB and TaS_3 , the mobilities around 100 K are $13 \text{ cm}^2/\text{V}\cdot\text{s}$ (Ref. 18) and $100 \text{ cm}^2/\text{V}\cdot\text{s}$ (Ref. 28), respectively. Thus, the mobility of the carriers in NbSe_3 over the type-III chains is relatively high. That is the reason why the conductivity jumps, as well as the hysteresis, are still distinguishable, though much smaller than the jumps in the lower CDW state.

IV. CONCLUSION

We have observed jumps of conductivity revealing single PS events for each of the two CDW states in NbSe_3 . The high mobility of carriers accompanying the lower CDW makes the steps below T_{P2} more visible ($\delta\sigma/\sigma$ achieves $\sim 1\%$), as well as the hysteresis in $\sigma(T)$. The analysis of the $\sigma(T)$ dependencies shows that the jumps provide switching between discrete conducting states. The jumps reveal the $q_2(T)$ dependence ($\delta q_2/q_2 \sim 10^{-4}$ in the temperature range 25–50 K) and provide the value of mobility of the carriers in the band relevant to the lower CDW state—the pocket holes.^{5,13} To our knowledge, this is the first direct measurement of the mobility of the carriers coupled with the type-I chains. The fast growth of mobility with decreasing temperature agrees with the model calculations for the pocket holes¹³ and, to be more precise, is even faster. While the $q_2(T)$ dependence, in

principle, could be observed directly with diffraction techniques, we do not see alternative direct methods of mobility determination.

The high mobility of the pocket holes (expected to be above $10^5 \text{ cm}^2/\text{V}\cdot\text{s}$ at 4.2 K) nominates NbSe_3 as an outstanding compound, not only within the CDW family. According to Ref. 29, the high mobility is the reason for low intralayer scattering. Therefore, the experiments on interlayer tunneling have allowed resolution of fine features in the energy spectra, such as the very narrow zero bias conductance peak.²⁹ The high mobility also allows the extreme quantum case in the Landau quantization to be achieved under relatively low magnetic fields.⁵

The steps of conductivity observed between T_{P1} and T_{P2} are much smaller ($\delta\sigma/\sigma \sim 0.1\%$). On their basis, we find the change of q_1 with T and the mobility of the quasiparticles on the type-III chains to be $400\text{--}500 \text{ cm}^2/\text{V}\cdot\text{s}$. The $q_1(T)$ variation appears to be several times weaker than the one obtained from the X-ray diffraction studies.²⁰

The single PS events appear to act as intrinsic injectors of “labeled” electrons or holes. On measuring the conductivity jump, we directly obtain the carriers’ mobility in that particular band. Therefore, the presence of the CDW provides the solution to a general problem topical for (semi)conductors with complex band structure.

Studies of the structure of conductivity steps not only reveal changes in the q -vectors, but they also give information on the fine structural effects, such as interaction of the two CDWs in NbSe_3 . One can also generalize the PS approach as a technique for structural and transport studies of mesoscopic samples of other types of compounds with incommensurate superstructure. As an example, we could mention single crystalline chromium—a spin-density wave system³⁰—where conductivity measurements could elucidate rearrangements of the antiferromagnetic domain walls.

ACKNOWLEDGMENTS

We are grateful to F. Lévy for supplying the high-quality samples, and to A. A. Sinchenko, V. F. Nasretdinova, I. G. Gorlova, and S. V. Zaitsev-Zotov for helpful discussions. The support of Human Capital Foundation (HCF), Russian Foundation for Basic Research (RFBR), and programs “New Materials and Structures” of the Russian Academy of Sciences (RAS) and of RAS Presidium (No. 27) is acknowledged. The work was performed in the framework of the Associated European Laboratory “Physical Properties of Coherent Electronic States in Condensed Matter,” including Departement Matière Condensée et Basses Températures (MCBT) and Kotel’nikov Institute of Radioengineering and Electronics of the Russian Academy of Sciences (IRE).

*Corresponding author: pok@cplire.ru

¹C. Brun, Z.-Z. Wang, P. Monceau, and S. Brazovskii, *Phys. Rev. Lett.* **104**, 256403 (2010).

²C. Brun, Z.-Z. Wang, and P. Monceau, *Phys. Rev. B* **80**, 045423 (2009).

³Y. Li, D. Y. Noh, J. H. Price, K. L. Ringland, J. D. Brock, S. G. Lemay, K. Cicak, R. E. Thorne, and M. Sutton, *Phys. Rev. B* **63**, 041103 (2001).

⁴J. Shen, X. Chen, Y. Zheng, H. Wang and Z. Xu, *J. Phys.: Condens. Matter* **15**, 5353 (2003).

- ⁵A. A. Sinchenko, R. V. Chernikov, A. A. Ivanov, P. Monceau, Th. Crozes, and S. Brazovskii, *J. Phys.: Condens. Matter* **21**, 435601 (2009).
- ⁶A. A. Sinchenko and P. Monceau, *Phys. Rev. B* **76**, 115129 (2007).
- ⁷Yu. I. Latyshev, P. Monceau, S. Brazovskii, A. P. Orlov, and T. Fournier, *Phys. Rev. Lett.* **96**, 116402 (2006).
- ⁸E. Slot, M. A. Holst, H. S. J. van der Zant, and S. V. Zaitsev-Zotov, *Phys. Rev. Lett.* **93**, 176602 (2004).
- ⁹S. V. Zaitsev-Zotov, *Uspekhi. Fiz. Nauk* **174**, 585 (2004) [*Physics-Uspekhi* **47**, 533 (2004)].
- ¹⁰E. Slot, H. S. J. van der Zant, and R. E. Thorne, *Phys. Rev. B* **65**, 033403 (2001).
- ¹¹J. Schäfer, M. Sing, R. Claessen, E. Rotenberg, X. J. Zhou, R. E. Thorne, and S. D. Kevan, *Phys. Rev. Lett.* **91**, 066401 (2003).
- ¹²P. Monceau, in *Electronic Properties of Inorganic Quasi-One-Dimensional Conductors*, Part 2, edited by P. Monceau (D. Reidel Publ. Comp., Dordrecht, 1985), p. 139.
- ¹³N. P. Ong, *Phys. Rev. B* **18**, 5272 (1978).
- ¹⁴N. P. Ong, and J. W. Brill, *Phys. Rev. B* **18**, 5265 (1978).
- ¹⁵G. Grüner, in *Density Waves in Solids* (Addison-Wesley, Reading, MA, 1994).
- ¹⁶D. V. Borodin, S. V. Zaitsev-Zotov, and F. Ya. Nad', *Zh. Eksp. Teor. Fiz.* **93**, 1394 (1987) [*Sov. Phys. JETP* **66**, 793 (1987)].
- ¹⁷S. G. Zybtsev, V. Ya. Pokrovskii, and S. V. Zaitsev-Zotov, *Nature Communications* **1**, 85 (2010).
- ¹⁸L. Forró, J. R. Cooper, A. Jánossy, and K. Kamarás, *Phys. Rev. B* **34**, 9047 (1986).
- ¹⁹S. V. Zaitsev-Zotov, *Synth. Met.* **55**, 2623 (1993).
- ²⁰A. H. Moudden, J. D. Axe, P. Monceau, and F. Levy, *Phys. Rev. Lett.* **65**, 223 (1990).
- ²¹D. Reagor, S. Sridhar, and G. Grüner, *Lect. Notes Phys.* **217**, 308 (1985).
- ²²M. P. Maher, T. L. Adelman, S. Ramakrishna, J. P. McCarten, D. A. DiCarlo, and R. E. Thorne, *Phys. Rev. Lett.* **68**, 3084 (1992).
- ²³J. McCarten, D. A. DiCarlo, M. P. Maher, T. L. Adelman, and R. E. Thorne, *Phys. Rev. B* **46**, 4456 (1992).
- ²⁴S. V. Zaitsev-Zotov, V. Ya. Pokrovskii, and P. Monceau, *Pis'ma Zh. Eksp. Teor. Fiz.* **73**, 29 (2001) [*JETP Lett.* **73**, 25 (2001)].
- ²⁵S. Aukkaravittayapun, K. A. Benedict, I. G. Gorlova, and S. G. Zybtsev, *Superecond. Sci. & Tech.* **8**, 718 (1995).
- ²⁶Typically, polynomial fits of the orders 6–15 were used.
- ²⁷S. V. Zaitsev-Zotov, and V. Ya. Pokrovskii, *Pis'ma Zh. Eksp. Teor. Fiz.* **49**, 449 (1989) [*JETP Lett.* **49**, 514 (1989)].
- ²⁸Yu. I. Latyshev, Ya. S. Savitskaya, and V. V. Frolov, *Pis'ma Zh. Eksp. Teor. Fiz.* **38**, 446 (1983) [*JETP Letters* **38**, 541 (1983)].
- ²⁹Yu. I. Latyshev, P. Monceau, A. A. Sinchenko, L. N. Bulaevskii, S. A. Brazovskii, T. Kawae, and T. Yamashita, *J. Phys. A: Math. Gen.* **36** 9323 (2003).
- ³⁰R. Jaramillo, T. F. Rosenbaum, E. D. Isaacs, O. G. Shpyrko, P. G. Evans, G. Aeppli, and Z. Cai, *Phys. Rev. Lett.* **98**, 117206 (2007); R. K. Kummamuru and Y.-A. Soh, *Nature* **407**, 859 (2008).